Review article

# High temperature sensible thermal energy storage as a crucial element of Carnot Batteries: Overall classification and technical review based on parameters and key figures

Alexej Paul [*], Felix Holy, Michel Textor, Stefan Lechner

*TH Mittelhessen University of Applied Sciences (THM), Institute for Thermodynamics, Energy Process Technology and System Analysis (THESA), Wiesenstrasse 14, 35390 Giessen, Germany*

## ARTICLE INFO

## ABSTRACT

Electricity storage is a key component in the transition to a (100%) $CO_2$-neutral energy system and a way to maximize the efficiency of power grids. Carnot Batteries offer an important alternative to other electricity storage systems due to the possible use of low-cost storage materials in their thermal energy storage units. The use of sensible storage material at high temperatures is of particular interest in order to achieve higher storage densities. A high number of research projects are currently being carried out in this field, and an increasing number of industrial players are also pushing the development of systems to market maturity, which results in a large variety of concepts. This work offers new approaches to the classification of Carnot Batteries and thermal energy storage systems. It gives an overview of the current state of the art in the field of thermal energy storage above 500 °C and compares the systems and concepts on the basis of key figures. The large number of concepts will inevitably be selected based on technical and environmental considerations. It is shown that solid and sensible thermal energy storage units can be represented as an efficient component of a Carnot Battery in the high temperature range. Total cycle energy efficiencies of ≥ 95% have been shown in literature. The 'fixed structure' design as a differentiation to the 'packed bed' is particularly well suited as it allows internal charging at temperatures greater than 1000 °C while minimizing charging losses.

## 1. Introduction

Many countries have set national targets [1] to expand renewable energy generation for various reasons such as the IPCC report [2]. Since solar and wind power is known to be fluctuating and thus often occurs outside the times of demand, generation must be decoupled from demand in terms of time. Electrification of all sectors and the use of electricity storage are important building blocks to achieve set goals and promote an energy transition [3]. Pumped hydro energy storage plants are the most widely used electricity storage systems. They are cheap and efficient. However, they are constrained by geographical conditions [4]. Chemical battery storage for grid stabilization has shown strong and continuous growth for years [5]. They are currently preferred, especially because of their high energy density, good efficiency, and last but not least, because they have no geographical constraints. However, they have higher specific costs than other storage technologies [4,6]. Carnot Batteries (CB) are novel electricity storage devices and have gained popularity in recent years. Unlike pumped hydro energy storage and chemical battery storage, CB are not yet mature enough for the market, but they can be a cost-efficient alternative [6–8]. Thermal energy storage units can provide an important contribution due to low-cost storage materials [9].

The aim of this work is to present a classification for CB and thermal energy storage (TES), to enable a simple classification. In addition, a comparison of demonstrators and theoretical concepts of TES devices will be presented based on characteristics from the literature, with a focus on high temperature applications and the use of solid and sensible storage materials.

Reviews of general energy storage systems such as Olabi et al. [10] and Das et al. [11] are available, providing overviews of energy storage technologies. Preliminary work in the field of CB is available by Dumont et al. [12] and Novotny et al. [13]. Both research groups have focused on CB as a unit. Esence et al. [14] have given a review with some TES in packed bed design. General requirements for TES with attention to the system and storage materials have been addressed by Gasia et al. [15]. The research groups Gil et al. [16] and Medrano et al. [17] have provided a two-part review on high temperature TES.
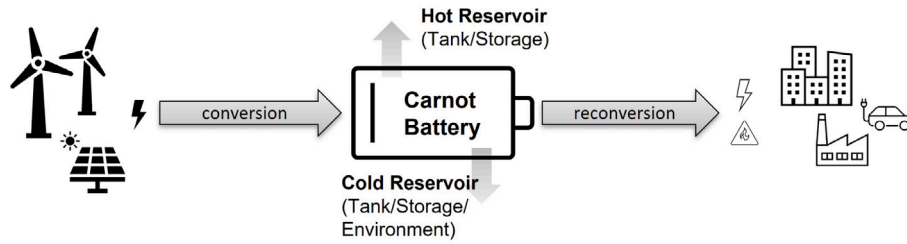
---

**Fig. 1.** Scheme of the general functioning principle of the electricity storage 'Carnot Battery'.
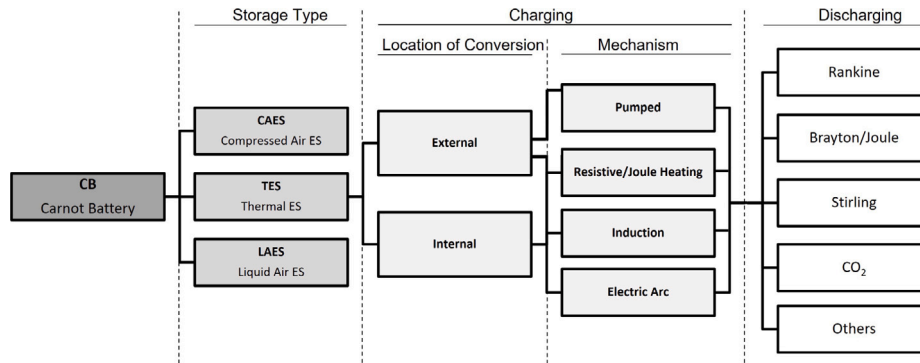


**Fig. 2.** Illustration of the proposed classification approach for carnot-batteries with a detailed path for carnot-batteries with thermal energy storages and subdivisions into charging and discharging methods.
*Source:* Adapted from [6,12,20] and extended.

In that review, concepts, materials, modeling, and case studies were considered in detail. The work of Liang et al. [18] elaborates in detail on the individual components of a CB, which have a major impact on the techno-economic evaluation. Currently, there is no review article that specifically addresses solid and sensible TES. That classifies them in terms of their operating temperature and as part of CB, while furthermore showing their potential in the higher temperature range. The present work aims to fill this particular gap.

## 2. Carnot Batteries

CB, also known as thermo-mechanical energy storage [6], are considered as electricity storage devices. They are characterized by their ability to store electricity at different temperature levels [12] (see Fig. 1). Thus, like other electricity storage systems, they can relieve the load on electricity grids, and some CB offer the possibility of coupling the heat and electricity sectors by extracting heat during discharging. Due to the existing potentials of CBs, since 2019 the 'IEA Energy Storage Task36', consisting of experts from academia and industry, is working on the dissemination and advancement of the research of this technology [19].

### 2.1. Classification of Carnot Batteries

Depending on the focus of the literature article, the technology on the first subdivision level is divided into the type of storage and then into the power generation process. In Dumont et al. [12], it is first subdivided by the type of storage and afterwards by the heat engine, first roughly into Brayton and Rankine, then finer into specific system configurations. Olympios et al. [6] and Steinmann [20] refer to CB as thermo-mechanical energy storage and follow a similar approach to Dumont's subdivision. They differ especially in the selection of systems in the first level of classification and generally classify CB in their used energy conversion process (e.g. Brayton or $CO_2$-cycle). Fig. 2 shows the classification of CB in Compressed Air Energy Storage (CAES), Liquid Air Energy Storage (LEAS) and the Thermal Energy Storage (TES)

Carnot Batteries. In addition to the common classification according to the discharging method, the charging method is proposed as a criterion. The charging technology has a significant influence on the efficiency and the temperature level of the TES within the CB (see Section 2.3).

### 2.2. Thermal energy storage

Thermal energy storage units cover a wide range of storage technologies and are applied in various fields. In general, they are used either as buffers to store thermal energy and relieve the load on heat generators or as regenerators for heat recovery. They have been used for decades in the building sector [21,23] and in industrial applications [24,25]. Another application area is power plants (conventional [26] as well as solar [27,28]) to optimize operating times. Currently, another area is being added as part of CBs. They serve as a hot or, in some CBs, also as a cold reservoir and represent an crucial part of this novel technology for storing electricity [12].

Since TES are based on different physical storage methods, this approach is often used in the literature to classify them. As shown in Fig. 3, a distinction is made between sensible, latent and thermo-chemical. The following designations for storage types can be derived from this:

- Sensible Thermal Energy Storage (S-TES)
- Latent Thermal Energy Storage (L-TES)
- Thermo-Chemical Energy Storage (TC-TES)

Subsequently, characteristics of the storages like the state of aggregation for sensible storages, the chemical assignment (e.g. organic) for latent storages or a finer physical subdivision for thermo-chemical TES will be distinguished. As mentioned before, S-TES are commonly used in many areas of everyday life and are therefore well researched for wide temperature ranges. Compared to L-TES and TC-TES, they have low storage density at the temperatures commonly used so far. However, L-TES and TC-TES are not yet commercially mature [14] and are more complex due to potential component corrosion, toxicity, and chemical instability.
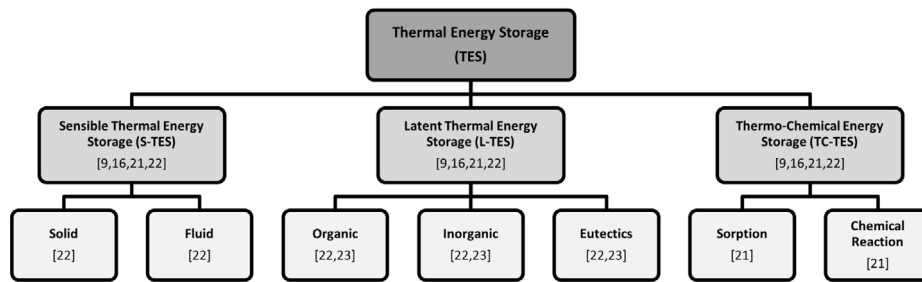
**Fig. 3.** Classification of thermal energy storage technologies from the literature.
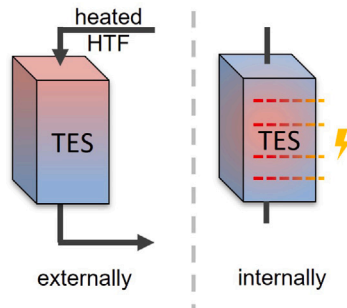*Source:* Adopted from [9,16,21–23].



**Fig. 4.** Illustration for the external (a) and internal (b) charging method as examples of the locations of energy conversion in Carnot Batteries.

### 2.3. Charging methods

The method of charging makes a significant difference in the technical design of a CB. Fig. 2 gives an overview of the classification of the charging technologies. Basically, a distinction can be made between the location of the energy conversion and the mechanism for charging the contained storage. The mechanism of charging is referred to the type of energy conversion and by the location, the determining aspect is whether the energy conversion takes place inside or outside the storage material (see Fig. 4).

For external charging variants, a heat transfer fluid (HTF) is required, which transports the supplied heat into the TES in the form of an enthalpy flow. Due to the forced flow, a fan is required to compensate for the pressure drop. The fan is usually placed between the TES and the heater and is thus limited by the outlet temperature of the TES. Research is being conducted at this point to achieve higher fluid temperatures during charging and thus higher maximum storage temperatures. These variants are flexible in terms of the charging mechanism and can therefore be designed in all shapes. Such a concept was implemented in Hamburg by Siemens Gamesa in their demonstrator 'ETES'. The storage material consists of volcanic rock and is externally charged by an electric resistance heater via an air flow (up to 750 °C). During discharging, the energy is transferred to a steam process by means of heat exchangers, thus converting the heat back into electricity [29]. The Solar Institute Jülich of the University of Applied Sciences, FH Aachen has developed and built a demonstrator (multiTESS) with a novel high-temperature resistance air heater (up to 1000 °C, externally heated) and is currently testing it in its own Brainenergy Park Jülich. The storage core consists of fine ceramic honeycombs [30,31].

In the special form 'pumped' of external charging methods, a heat pump process is used to 'pump' the heat from a lower temperature level (ambient heat, cold TES or waste heat) to a higher temperature level with additional electrical auxiliary energy (e.g. mechanical compression). CB, fitting into this category are also called pumped thermal energy storages (PTES). They essentially contain two TES (e.g. packed bed or water reservoirs) and a heat pump-like system for charging,

as well as a heat engine (HE) for power generation and, optionally, heat exchangers for the input/output of heat and/or cold. From the current point of view, these CB can only be charged externally. Robinson [32,33] does show a conceptual design using solid and liquid metals as storage materials for internal charging according to the heat pump process up to above 1500 °C, but this heat pump technology is still far from practical application. PTES systems can use external heat sources (such as ambient heat) during charging, but are limited in their maximum outlet temperature. They therefore tend to be operated in the lower temperature range (<200 °C). The MAN company offers a CB called Electro-Thermal Energy Storage System, or 'ETES' [34], with a $CO_2$ heat pump, a $CO_2$ Rankine process and water storage tanks. Benato et al. [35] modeled and investigated a theoretical concept based on gas turbines and bulk (packed bed) storage with air as working medium. This type of CB is also called Brayton Battery due to the utilized electricity generation process. It allows higher temperatures of 500 °C or more [12] and also belongs to PTES.

If the charging unit is shifted into the storage, the losses in transmission during charging are reduced considerably and an external charging unit becomes dispensable. Peng et al. describe an internally charged concept, where the storage material (ceramic with the addition of graphite) is electrically conductive and thus should be heated to temperatures above 1100 °C via Joule heating [36]. Likewise, internally charging offers the possibility of integrating resistive heating elements within the storage unit [7,36]. Since no HTF needs to be heated, temperatures greater than 1000 °C can be achieved easily, but the use of ambient heat is excluded in a purely internal charging. At the University of Applied Sciences - TH Mittelhessen, such a demonstrator ('High-T-Stor') has been built and investigated until the end of 2020. The storage consists of a masonry assembly of ceramic bricks. Charging is possible up to 1100 °C via resistive heating elements integrated in the storage. During discharging, the energy is released to an air flow and converted to electricity in an inverse gas turbine process [37]. A new, more advanced demonstrator is currently under construction and will start test operation in early 2023. It differs mainly in an optimized core geometry with an improved insulation concept and an externally fired gas turbine [38] process for electricity generation [39]. Theoretically, there are further possibilities for charging the storage, e.g. via an electric arc or by induction. So far, no such concepts or implemented storage systems are known.

### 2.4. Discharging methods

The discharge process of the storage unit has a decisive influence on the efficient and economical operation of the CB. A HTF flows through the TES and absorbs the stored heat, supplying a reconversion process. High electrical reconversion efficiency, i.e., the ratio between the electrical power generated and the thermal power required by the TES, is the primary goal. To increase the overall efficiency, additional useful heat can be extracted from the process, for example for district heating or process heat. Regarding the method of discharging, a temperature range is often already limited by the method of charging, which makes
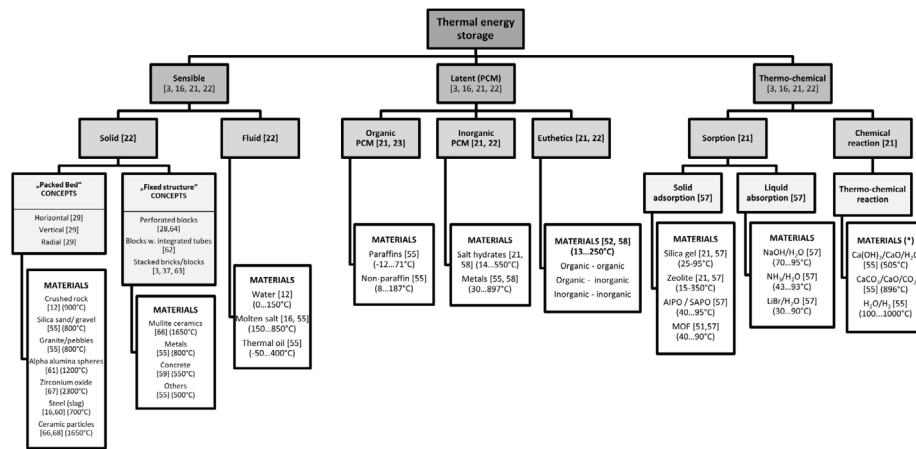
**Fig. 5.** Classification of thermal energy storage technologies with design concepts and used materials.
*Source:* Adopted from [9,16,21–23] and extended by [12,28,29,37,51,52,55–68].

a distinct discharging technology predestined for utilization. The common electricity generation processes from Fig. 2 are the steam power process (Clausius Rankine cycle), see [29,40], the organic Rankine cycle [41] and the (supercritical) $CO_2$ process, see [15,34,42,43].

A large number of adapted gas turbine processes (Brayton or Joule cycle) for heat recovery in a CB can be found in the literature, see [44–47]. In Holy et al. [38] five process variants (for cogeneration) are described, in which the HTF fluid flows through the TES pressureless (atmospheric) and is partially used in the coupled gas turbine process. For this purpose, air can be selected as the working medium of the gas turbine as well as the HTF in the TES, making possible leakages in the plant system uncritical. The components of the gas turbine process are comparatively inexpensive, which favors the economic viability of CB. In addition, there are processes still under development, such as the liquid-air process [20,48] and the multi-junction photovoltaic cell, also known as thermal photovoltaic (TPV) [36,49]. Processes like these, which cannot be assigned to one of the groups mentioned before, are grouped as 'Others' in Fig. 2.

## 3. Technical assessment of sensible thermal energy storage

### 3.1. Design types of solid S-TES

Fig. 5 gives an overview on the classification of sensible thermal energy storages (S-TES). The solid S-TES are explained in the following. Liquid S-TES are not the focus of this work, because they are well known in the temperature range up to 600 °C especially due to their application in solar power plants and represent the state of the art. See [12,15,22,50] for further information. For the two other storage classes L-TES and TC-TES, reference is made here to the existing literature [16,51–54].

The design of a S-TES is essential as it affects many conditions such as the distribution of the HTF in the storage. It is important to mention the differentiation from the common and often used 'packed bed' design of S-TES by the new definition of 'fixed structure' storages in order to account for the designs without a packed bed. This includes concrete storage [27,63,69–72] or storage with stone or slab stacking [7,28,37, 39,59,73–77].

TES of the **packed bed** (PB) design can be filled with a wide range of materials. An important requirement is a sufficient resilience to cycle-related degradation [78]. Therefore, low-cost, because locally available, materials such as volcanic rock [29,79,80], sand or fine rock fills [81,82], or also waste materials such as metal slag granules from steel production [60] can be used. The literature also contains investigations with fills made of aluminum oxide granulate [61,83].
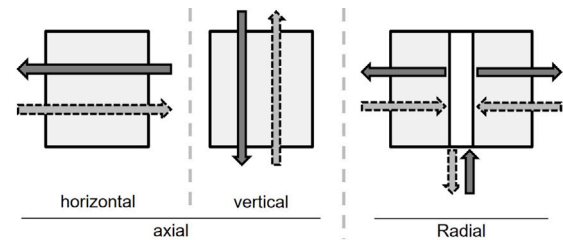


**Fig. 6.** Visualization of the main flow direction in thermal energy storage systems based on the packed bed concept.
*Source:* Adapted from [29,84].

The type of air distribution within a storage unit describes the main flow direction of the fluid as it passes through the storage material. According to Odenthal [84], it can be divided into axial and radial. Von der Heyde and Schmitz [29] distinguished the axial airflow into horizontal and vertical. Krueger et al. [85] consider also a meander shaped form of flow. Summarizing the first two approaches results in three possible flow directions. Two axial directions (horizontal and vertical) along the storage axis and one radial direction from the inside to the outside, see Fig. 6.

Detecting the actual solid state temperature and thus the state of charge or SOC for short (see Eq. (11)) of the storage unit is difficult in a PB TES. Temperature sensors that are inserted only into the bulk run the risk that they mainly detect the fluid temperature. Klein et al. [68] presented a possibility to circumvent this problem. In this case, temperature sensors were installed in individual grains of the bed. However, this requires a sufficiently large grain size of the storage material to be able to locate the measuring tip inside of it.

Non-bulk storage systems are characterized by a fixed internal structure that contains shaped flow channels. For this reason they are also referred to here as **fixed structure** (FS) TES. Due to the complex but necessary shaping, they are generally associated with higher investment costs than packed bed storage systems. In return, the shaping brings flexibility in the form of free design of the core geometry through its manufacturing process. Wall thicknesses and hydraulic diameters of the flow channels can be influenced by the geometry. The use of mass-produced molded bricks such as perforated [28,65] or common masonry bricks [7,37], as well as slabs [74], can reduce the cost of shaping. In the field of concrete storages, Laing et al. [69] and Hoivk et al. [71] have presented demonstrators that incorporate cast-in pipes to prevent contact of HTF and storage material. Cavities for internal heating (heating channels) can also be provided directly as implemented in Lechner et al. [37] or presented by Stack et al. [7].
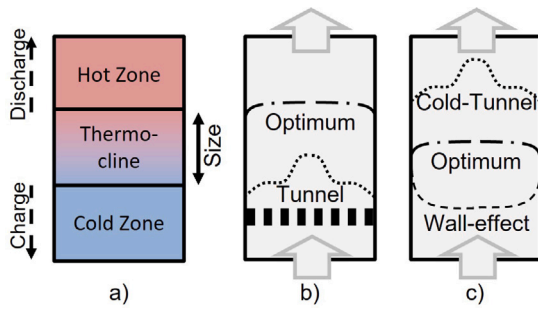
**Fig. 7.** Illustration of thermal stratification issues associated with the thermocline (a) and tunneling effects for fixed structure TES (b) and fixed bed TES (c). The dashed lines in (b) and (c) represent the uniformity of the velocity distribution for different cases.



**Fig. 8.** Temperature profile and distribution of usable and unusable thermal capacity within the sensible thermal energy storage along the main flow direction for charging and discharging.

### 3.2. Thermal stratification

The temperature gradient within the storage is an indication of the efficiency of the charging/discharging process, as it allows some conclusions to be drawn about the usable portion of the storage capacity. Three zones can be defined for the storage. Two zones with high and low temperatures, respectively, and negligible temperature gradients, and one zone with a significant temperature gradient, the so-called thermocline, see Fig. 7.

The shape and size of it depends not only on system parameters (e.g. mass flow, temperatures) or geometric aspects (e.g. hydraulic diameter, free flow cross-section), but also on the charging and discharging methods used. The depth of charging and discharging during thermal cycles also influences the development of it, which is of particular importance in part-load operation. For externally charged TES the thermocline moves back and forth between the hot and cold ends of the storage during the thermal cycles. It is often avoided to charge the storage completely, because the outlet temperature rises towards the end of the process and thus the charging efficiency decreases [79,86]. In the case of internal charging, the thermocline disappears when the storage is fully charged and reforms when it is discharged. With a larger expansion of this zone, the storage can also be discharged less deeply, because the usable temperature is undercut earlier, although the average capacity of the storage has not yet cooled down completely. For this reason, the shape of the thermocline is a decisive factor in determining how far the storage can be charged or discharged and thus also the proportion of the unusable capacity. Fig. 8 schematically shows the share of usable capacity $C_{usable}$ as well as the non-usable shares during charging $C_{ch, loss}$ and discharging $C_{dis, loss}$. The total (nominal) thermal capacity $C_{nom}$ describes the sum of the usable and non-usable thermal capacity and spans the nominal temperature range between $T_{min}$ and $T_{max}$:

$$C_{nom} = C_{usable} + C_{ch, loss} + C_{dis, loss} \tag{1}$$

$T_{min}$ describes the inlet temperature into the TES during discharging and thus represents the minimum storage temperature during cyclic operation (heat losses are not taken into account). The charging process can be operated until the storage tank temperature at the outlet drops below a critical limit $T_{min, dis, out}$. Below this point, the outlet temperature of the enthalpy stream is too low for a reasonable operation of the subsequent reconversion or heat extraction.

$T_{max}$ defines the upper temperature limit of the TES, which in externally charged concepts corresponds to the inlet temperature during the charging phase. The outlet temperature during charging can be a limiting factor for the external charging unit, which is described by the limit temperature $T_{max, ch, out}$. Storage units with integrated (internal) charging units are not flown through and therefore have an advantage during the charging process. They can be fully charged and the capacity
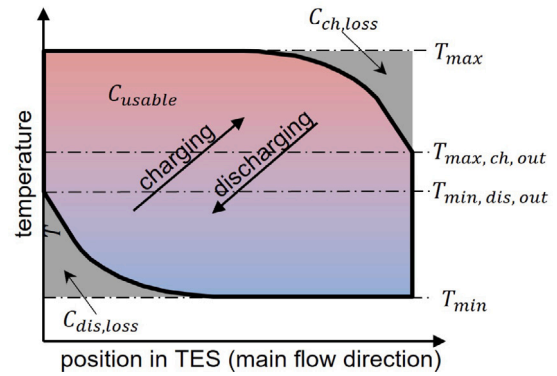
losses during charging (charging losses) can be largely avoided by the internal charging. The additional volume required for charging a FS storage unit, which therefore represents unusable capacity, is already taken into account by the void volume $V_{void}$ and thus also the key figure of the void fraction due to the additional space required by the charging unit in the storage unit (see Eq. (7)). In the case of PB storage units, the share of unused capacity during charging is difficult to estimate because, as in the case of discharging, it depends strongly on the operational management.

The usable capacity ratio $\Phi$ (see Eq. (2)) has been established as a classification of storage utilization [29]. It has also been called 'material efficiency' by Ortega-Fernandez et al. [60] and 'utilization rate' by Bruch et al. [87].

$$\Phi = \frac{C_{usable}}{C_{nom}} \tag{2}$$

At idle, a homogenization of the temperature layers due to internal heat transfer can generally be assumed for thermal storages. This effect is driven by the heat transfer within the storage material. It occurs in general as a combination of conduction, convection and radiation. In packed beds, in particular at high temperatures, the radiation component between the grains dominates, which can be accounted for by a temperature-dependent effective thermal conductivity [86,88]. FS TES are particularly determined by heat conduction. In both cases heat transfer between solid and fluid becomes more important when liquid HTFs are used, as the heat transfer improves significantly [14].

The problem of deviations from the optimal plug flow cannot be neglected for the stratification within STES (cf. Fig. 7b and c). This results in a non-uniform distribution of the flow within the storage material. In the case of FS storage units, this is caused by the geometry given by the shaping. Directly adjacent flow channels are preferred over distant ones, which is significantly influenced by the hydraulic diameter (see Eq. (3)) of the flow channels. A is the cross-sectional area and P is the wetted perimeter of the flow.

$$D_h = 4\frac{A}{P} \tag{3}$$

In PB storage units, the volume change of the grains during thermal cycles can lead to channel formation within the bed. This occurs especially in the boundary area ("wall effect") and can be reduced by flexible internal insulation [79]. A downward tapering geometry of the storage like a turncated cone [89] or a hemisphere [80] prevents this effect due to the geometry-related vertical movement of the grains. Another topic is the cold tunnel effect, which was investigated by Davenne et al. [90]. In this case, during the discharging of PB S-TES, a 'cold tunnel' occurred in the middle of the bed, which was caused by the coarseness of the bed, i.e. a high void fraction. This effect may also appear in FS storage units due to a too big hydraulic diameter of the flow channels.
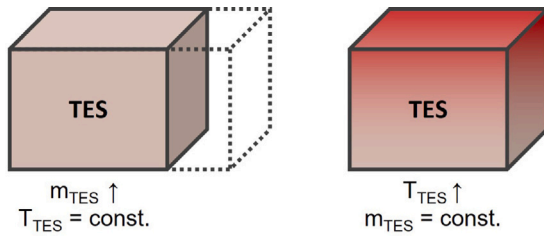
**Fig. 9.** Options of capacity expansion for sensible thermal energy storages.

### 3.3. Operating temperature

The operating temperature range of the TES affects the selection of the storage material, as they can decompose or experience an undesirable phase change. Material properties of the storage materials are temperature dependent and can have a major impact on storage behavior, especially for large temperature changes.

According to Eq. (4), there are two ways to increase the stored internal energy of STES without changing the storage material (see Fig. 9).

$$E_{th} = \Delta U_{TES} = \int_0^{V_{TES}} \rho_{mat} (1 - \epsilon) \left( u \left( T_{ref} \right) - u \left( T_{TES} \right) \right) dV \qquad (4)$$

In addition to increasing the volume and thus also the mass, which is also common for other types of storage, if thermal load limits of other components are neglected, the upper (operating) temperature and thus the temperature range can be increased for S-TES. The volume and the price per m³ of storage material remain constant, which increases the energy density and decreases the specific price per stored kWh. For this reason, the use of S-TES is more effective at higher temperatures due to the larger possible temperature differences and it is worthwhile to differentiate the storage units according to the (maximum) operating temperature.

In the literature, some approaches can be found and split into 'low', 'medium', 'high' and also 'sub-zero' and 'ultra-high'. Fig. 10 shows the proposed approach in comparison with the literature. Kronhardt et al. [91] proposed in 2014 that the range for medium temperature storages should be $100 < T < 500$ °C. Below that (<100 °C) is the Low Temperature range and above it (>500 °C) the High Temperature range. Other approaches are based on aquiferous systems, for example, which is why the limit for 'high' was set at 120 °C [22] or 150 °C [15]. Facing the increased number of storages also in this range, a new approach that stretches the lower ranges and subdivides the upper one is useful. Considering the division proposed here, TES units can be designated as follows:

- SZT-TES for sub zero temperature range
- LT-TES for low temperature range
- MT-TES for medium temperature range
- HT-TES for high temperature range
- UHT-TES for ultra high temperature range

Analogously, sensible thermal energy storage in the high temperature range can be called high temperature sensible thermal energy storage or HTS-TES. Since in the high and ultra-high ranges there can be a higher temperature level in the storage than that of the process of energy utilization (e.g. HE), the process control may require a special circuit (e.g. bypass) that lowers the outlet temperature to the required level. This increases the discharging time of the storage, avoids thermal overload of the reconversion process and components, and still utilizes the higher temperature level of the TES. From an exergetic point of view, however, an attempt should be made to use the highest available temperature in the TES for efficient discharging [38].

### 3.4. Thermal characteristics and key figures

In order to be able to compare different storages parameters are given to describe essential properties of the S-TES technology. In addition to the absolute values such as the nominal storage mass,

$$m_{TES} = V_{TES} (1 - \epsilon) \rho_{mat} = V_{mat} \rho_{mat} \qquad (5)$$

the nominal storage capacity

$$C_{nom} = V_{TES} \rho_{mat} (1 - \epsilon) \int_{T_{min}}^{T_{max}} c_{mat} (T) dT \, dV_{TES}$$

$$\approx m_{TES} \bar{c}_{mat} \Delta T_{nom} \qquad (6)$$

and charging power $Q_{th,ch}$ as well as discharging power $Q_{th,dis}$, the specific values are particularly important as they increase comparability. Here, $\rho_{mat}$ is the density of the storage material, $V_{mat}$ is the volume of the storage material (without the void), and $V_{TES}$ is the total volume of the storage (without insulation). The so-called void fraction or porosity $\epsilon$ (see Eq. (7)) can be used to evaluate the compactness or bulk density. It thus represents the utilization of the available space and corresponds to the ratio of void volume to storage volume. The higher this value, the lower the utilization.

$$\epsilon = \frac{V_{void}}{V_{TES}} = 1 - \frac{V_{mat}}{V_{TES}} \qquad (7)$$

The nominal operating temperature or the operating temperature range $\Delta T_{nom}$ of the storage determines the maximum energy density for STES. This does not refer to the material-specific limit temperature, but to the maximum operating temperature specified in literature. The declared nominal storage capacity and the storage volume, results in the often-used nominal volumetric storage capacity

$$c_{nom,vol} = \frac{C_{nom}}{V_{TES}}. \qquad (8)$$

For better comparability, the specification of a volumetric heat capacity (see Eq. (9)) is important, since it is not dependent on the declared temperature difference and thus better reflects the potential of the storage technology.

$$\bar{c}_{TES,vol} = \rho_{mat} \bar{c}_{mat} (1 - \epsilon) \qquad (9)$$

One of the most significant figures for processes is the efficiency. For thermal storages, the maximum cycle efficiency can be used, which represents the storage efficiency. Geissbühler et al. [93] call it 'cycle energy efficiency of the TES' and relate the energy stored during charging $E_{th,c}$ and the energy extracted during discharging $E_{th,d}$ from Eq. (4).

$$\eta_{TES} = \frac{E_{th,d}}{E_{th,c}} = \frac{\Delta U_{TES, d}}{\Delta U_{TES, c}} \qquad (10)$$

By defining the stored thermal energy (see Eq. (11)), it is also possible to calculate the dimensionless state of charge (SoC) for the storage. For this purpose, the thermal energy is related to the nominal storage capacity (from Eq. (6)).

$$SoC_{TES} = \frac{E_{th}}{C_{nom}} \qquad (11)$$

Another important parameter is the pressure drop across the storage. It is strongly dependent on the hydraulic diameter, the free cross-section area and the design mass flow. For FS TES, it is often easy to determine using popular relations, such as the Hagen–Pioseuille law [94] in the laminar flow case, because the flow cross-sections in the storage have simple geometries (rectangular/circular). For PB TES, empirical approximation formulas such as the Ergun Equation [95] are used, since the bulk in the storage has a complex geometry.

## 4. Overview of H-STES demonstrators and concepts

This chapter gives an overview of current HTS-TES in their respective development status, from theoretical concept to pilot-scale (also called prototype-scale) found in literature and industry. The storage
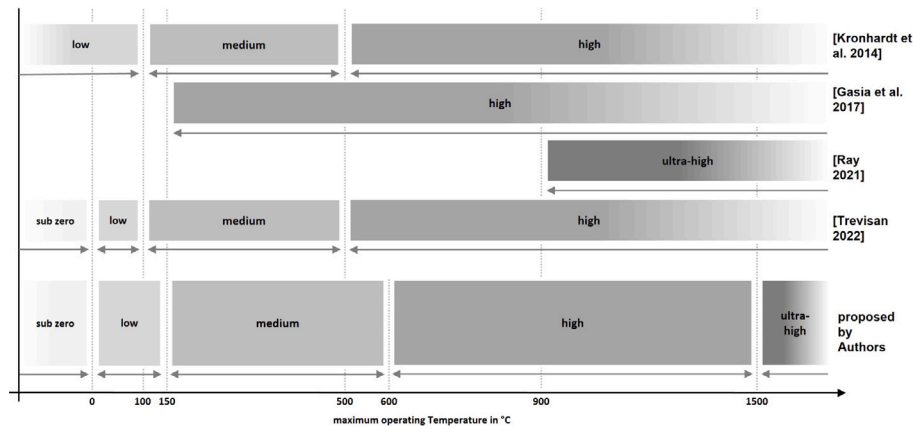
**Fig. 10.** Definition of limit temperatures of the proposed subdivision scale for operating temperature ranges of energy storage systems [15,53,91,92].

systems are classified on the basis of specifications or the available information in literature about them:

- 0: Theory
- 1: Lab-scale
- 2: Demonstrator-scale
- 3: Pilot-scale

'Theory' stands for a concept or a theoretically considered storage, which may be based on existing facilities (e.g. large scale-up), but has not been built yet. If a small facility has already been built in a laboratory environment, it is considered onward as 'lab-scale'. As soon as a storage plant has been built for demonstration purposes, it is a 'pilot' or 'demonstrator' plant. The distinction between the two can only be made on the basis of the boundary conditions and therefore the transition can be seamless [13]. Therefore, for this review, the declaration of the scale is taken from the corresponding literature source and is independent of the associated capacity. Pilot-scale or prototype plants are close to the sizing for their intended use, as defined by the Technology Readiness Level [96], and are tested extensively in their intended application environment.

Within TES technology, many combinations of material and design are possible. The fields of application of the storages can also be diverse, as already described in Section 2.2. An overview of the collected S-TES is given in Tables 1–3. The Tables 1 and 2 list non-commercially developed S-TES in PB (Table 1) as well as FS (Table 2) design types and Table 3 lists commercially developed S-TES only. They are mostly either storages as an element of a CB for electricity storage, heat storages in power plants (especially CSP) to optimize operation times or regenerators for pure heat recovery in industrial processes. Markings are included in the summary tables to highlight particular data. The collected data is partially incomplete due to gaps in published information. Values marked with an [a] were calculated (without own assumptions) from other data and missing data are marked with 'not available', in short 'n.a.'. The calculated nominal capacity (see Eq. (6)) is based in that case on the declared operating temperature difference (see Table A.4 in appendix) of the corresponding authors.

Table 1 shows PB STES with specified maximum storage temperatures above 500 °C. It is noticeable that, with the exception of one STES, all storage units are externally charged and most have the typical buffer storage geometry of a cylinder filled with rocks with a vertical flow. A storage unit presented by Arakoohsar and Andresen [107] cannot be assigned unambiguously to the charging method. Some other storages have a cubic shape [79,95,100] and only a few have a completely different geometry such as a truncated cone [89,102,105], a hemisphere [80] or a sliced half-cylinder [93]. Two HTS-TES stand out with horizontal [79] and radial main flow directions [86]. In other storages alpha alumina [35], magnetite [104], metal slags [60], ceramic

granulates [68,108], silica sands [8,81,82] or zirconium oxide [106] were used.

A list of FS STES is given in Table 2. These concepts usually use an external charging method and different kinds of ceramic storage material such as solid fire bricks [7,37], perforated ceramic bricks [28], fireclay slabs [95], or cast molded bricks [39], and the shape of the storage is usually a cuboid. The preferred main flow direction is also vertical, only the planned storage in the FlexQuartier Gießen stands out with a horizontal flow direction [39]. The charging of the storage with internal location of energy conversion is realized either via resistance heating elements integrated in the storage [7,37,39] or by electric conductive storage material itself [119].

Table 3 shows a list of commercially developed HTS-TES. Due to incomplete information from the companies, only a few of these systems are included in the comparisons (Figs. 11 and 12). There are about twice as many PB S-TES as FS S-TES. Among these, almost all PB storages have sand or stone fills and FS storages are mainly utilizing with ceramic storage material. Among the commercially developed storages, the cubic design dominates with twice the number of storage units, compared to the cylindrical design. The main flow direction is equally split between horizontal and vertical. Two storage systems stand out here. These are the storage systems of STORASOL GmbH [8, 110] with radial airflow between individual thin-layer storage modules and the theoretical concept of Antora Energy [119], which does not use airflow at all. Here, the storage is charged direct electrically (internally) and is discharged by TPV modules, which are still under development and can be moved into the storage as needed to convert the thermal radiation into electric power [49]. For charging and discharging, the 'ENDURING' storage from the National Renewable Energy Laboratory (NREL) deserves special mention because the storage material itself is moved. For charging, it is trickled through a novel charging module and heated therein. For discharging, a fluidized-bed heat exchanger releases the stored energy to a secondary air flow, that drives a gas turbine process and then returns the storage material to the container [117].

A total of 44 storages were listed, of which 12 represent theoretical concepts, 18 are in commercial development, and only 9 have already reached pilot plant status (see Table A.4). The rest is still in the development and testing process (lab- or demonstrator-scale). In conclusion, it can be stated that the most commonly studied types of S-TES are the externally charged PB storage. There remains a need for research on storage systems with FS, since they have rarely been considered in the high temperature range and also because they can be constructed with an internal charging unit. Among the storage plants with the largest storage capacity is the pilot plant of Bren Miller with 200 MWh [114] thermal capacity. The ETES demonstrator of Siemens Gamesa and the theoretical scale-up concept of Zanganeh have capacities of respectively 130 MWh [120] and 3.6 GWh (for each storage) [102].

**Table 1**

Overview of solid PB HTS-TES from the literature sorted by ascending capacity.

| Source | Scale | $T_{max}$ | Energy conversion | Shape | Main flow direction | Storage inventory | $\bar{c}_{TES,vol}$ | $C_{nom}$ | $\eta_{TES}$ |
|---|---|---|---|---|---|---|---|---|---|
| [-] | [-] | [°C] | [-] | [-] | [-] | [-] | [Wh/(m³K)] | [MWh] | [-] |
| [61,97] | 1 | 700 | externally | cylinder | vertical | alpha alumina | 685[a] | 5.4E-05[a] | n.a. |
| [98,99] | 1 | 700 | externally | cylinder | vertical | crushed steatite | 477[a] | 9.8E-04[a] | 0,90 |
| [68] | 1 | 900 | externally | cylinder | vertical | Denstone ceramicpebbles | 423[a] | 2.9E-02[a] | n.a. |
| [92] | 1 | 1000 | externally | cylinder | radial | alpha alumina | 484[a] | 5.0E−02 | 0.72 |
| [100] | 1 | 530 | externally | cuboid | vertical | rocks (dolerite) | 453[a] | 0.40 | n.a. |
| [79] | 1 | 600 | externally | cuboid | horizontal | rocks | 441[a] | 0.45 | 0.68 |
| [80] | 2 | 600 | externally | hemi-sphere | vertical | crushed rocks | 411[a] | 1.00 | 0.81 |
| [60] | 2 | 900 | externally | cylinder | vertical | EAF steelslag pebbles | 526[a] | 1.05 | n.a. |
| [95] | 3 | 800 | externally | cuboid | vertical | basalt pebbles | 502[a] | 1.42 | n.a. |
| [93,101] | 3 | 550 | externally | modifiedhalf cylinder | vertical | crushed rock | 508[a] | 12.0 | 0.91 |
| [35] | 0 | 550 | externally | cylinder | vertical | alpha aluminaspheres | 720[a] | 26,98[a] | 0.67 |
| [102] | 0 | 550 | externally | modifiedturncated cone | vertical | rocks | 434[a] | 100.0 | 0.89 |
| [103] | 0 | 677 | n.a. | cylinder | vertical | rocks | 403[a] | 124.0[a] | 0.86 |
| [104] | 0 | 500 | externally | cylinder | vertical | magnetite particles | 754[a] | 160.0 | 0.88 |
| [26] | 0 | 900 | externally | cylinder | vertical | EAF steelslag pebbles | 533[a] | 2210.0 | n.a. |
| [89,102] [105] | 0 | 650 | externally | modifiedturncated cone | vertical | rocks | 437[a] | 7200.0 | 0.95 |
| [106] | 1 | 1100 | externally | cylinder | vertical | zirconium oxidepallets | n.a. | n.a. | n.a. |

[a] - Calculated value.

**Table 2**

Overview of solid FS HTS-TES from the literature sorted by ascending capacity.

| Source | Scale | $T_{max}$ | Energy conversion | Shape | Main flow direction | Storage inventory | $\bar{c}_{TES,vol}$ | $C_{nom}$ | $\eta_{TES}$ |
|---|---|---|---|---|---|---|---|---|---|
| [-] | [-] | [° C] | [-] | [-] | [-] | [-] | [Wh/(m³K)] | [MWh] | [-] |
| [94] | 1 | 680 | externally | cuboid | vertical | ceramic honeycomb bricks | 341[a] | 1.8E-02[a] | n.a. |
| [74] | 1 | 530 | externally | cuboid | vertical | ceramic plateswith cutouts | 569[a] | 1.9E-02[a] | n.a. |
| [94] | 1 | 680 | externally | cuboid | vertical | ceramic honeycomb bricks | 179[a] | 7.1E-02[a] | n.a. |
| [95] | 3 | 800 | externally | cuboid | vertical | ceramic plates | 417[a] | 1.11 | n.a. |
| [37] | 2 | 1100 | internally | cuboid | vertical | massive ceramicbricks | 521[a] | 1.51[a] | n.a. |
| [74] | 0 | 650 | externally | cuboid | vertical | ceramic plateswith cutouts | 569[a] | 4.00 | n.a. |
| [39] | 0 | 1200 | internally | cuboid | horizontal | ceramic plateswith cutouts | 549[a] | 4.78 | 0.9 |
| [28] | 2 | 680 | externally | cuboid | vertical | alumina porcelain,honeycomb bricks | 205[a] | 8.60 | n.a. |
| [7] | 0 | 1600 | internally | n.a. | vertical | massive ceramicbricks | 698[a] | 250.0 | n.a. |

[a] - Calculated value.

**Table 3**

Overview of commercially developed solid HTS-TES from the literature sorted by ascending capacity.

| Source | Scale | $T_{max}$ | Energy conversion | Shape | Main flow direction | Storage inventory | $C_{nom}$ | $\eta_{TES}$ | Storage design |
|---|---|---|---|---|---|---|---|---|---|
| [-] | [-] | [° C] | [-] | [-] | [-] | [-] | [MWh] | [-] | [-] |
| [109] | 1 | 900 | externally | cylinder | horizontal | waste refractoryceramics | 0.08 | n.a. | n.a. |
| [108] | 1 | 1000 | externally | cylinder | vertical | ceramic packedbed material | 1.00 | n.a. | PB |
| [31] | 2 | 1000 | externally | cuboid | vertical | ceramic honeycombs | 1.40 | 0.80 | FS |
| [8,110] | 2 | 600 | externally | cuboid | radial | small grained silicasand, multiple thin PB modules | 1.50 | n.a. | PB |
| [109] | 3 | 1000 | externally | cuboid | horizontal | waste refractoryceramics | 2.00 | 0.95 | n.a. |
| [76] | 3 | 650 | externally | cuboid | horizontal | steel rods | 2.40 | n.a. | FS |
| [81] | 3 | 1300 | externally | cuboid | vertical | high temperatureconcrete granulate | 4.20 | n.a. | PB |
| [111] | 2 | 800 | externally | cuboid | horizontal | crushed rock | 5.00 | 0.95 | PB |
| [112,113] | 2 | 500 | externally | cylinder | vertical | crushed rock | 16.00 | 0.97 | PB |
| [114] | 3 | 750 | externally | cuboid | horizontal | crushed rocks | 200.0 | n.a. | PB |
| [29,115] | 2 | 800 | externally | cuboid | horizontal | crushed volcanic rock | 130.0 | n.a. | PB |
| [116] | 3 | 1000 | externally | cuboid | vertical | sands | n.a. | n.a. | PB |
| [117] | 0 | 1200 | externally | cylinder | vertical | silica sands | n.a. | n.a. | PB |
| [118] | 3 | 600 | externally | cylinder | vertical | crushed rocks | n.a. | n.a. | PB |
| [82] | 2 | 1000 | externally | cuboid | horizontal | silica sand | n.a. | n.a. | PB |
| [75] | 0 | 2000 | internally | cylinder | vertical | ceramic honeycombcowperstones | n.a. | n.a. | FS |
| [119] | 0 | 1500 | internally | cuboid | none | graphite blocks | n.a. | n.a. | FS |
| [72] | 2 | 600 | externally | cuboid | horizontal | high temperatureconcrete with inner tubes | n.a. | n.a. | FS |

[a] - Calculated value.

As described in Section 3.3, S-TES are particularly worthwhile in the high temperature range. In Fig. 11 storage units with particularly high energy density potential are located in the upper and right-hand areas. It is clearly visible that most of the storage units are in the area of transition from 'medium' to 'high' and at the beginning of the high temperature range. Most of these plants show a volumetric heat capacity of 300 to 600 Wh/(m³ K). The distribution in the vertical direction depends strongly on the density of the storage material, since the specific capacity for most materials is in the approximate area around 1000 J/(kg K) and the density varies strongly. Only the systems of Zunft et al. [28] and Li et al. [94] are around 200 Wh/(m³ K) and the theoretical concepts of Mc Tigue et al. [104] or Benato [35] are above 700 Wh/(m³ K). The latter two concepts have their high values, due to their significant higher indicated density of the used storage material of almost 4000 kg/m³ and even more than 5000 kg/m³, respectively. This raises the energy density potential significantly, as the other storages are in the range of 2000–3000 kg/m³. In the range above 1000 °C maximum storage temperature, only a few storages can be found.
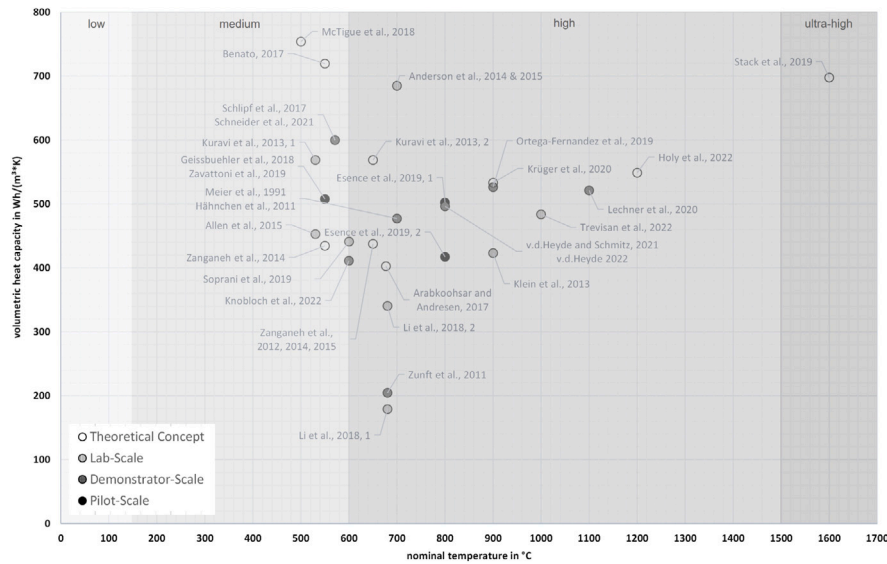
**Fig. 11.** Volumetric heat capacity and nominal temperature for the reported HTS-TES [7,8,26,28,35,37,39,60,61,68,74,79,80,86,89,93–95,97–105,110,115] in their temperature field and with corresponding markings for the development level.
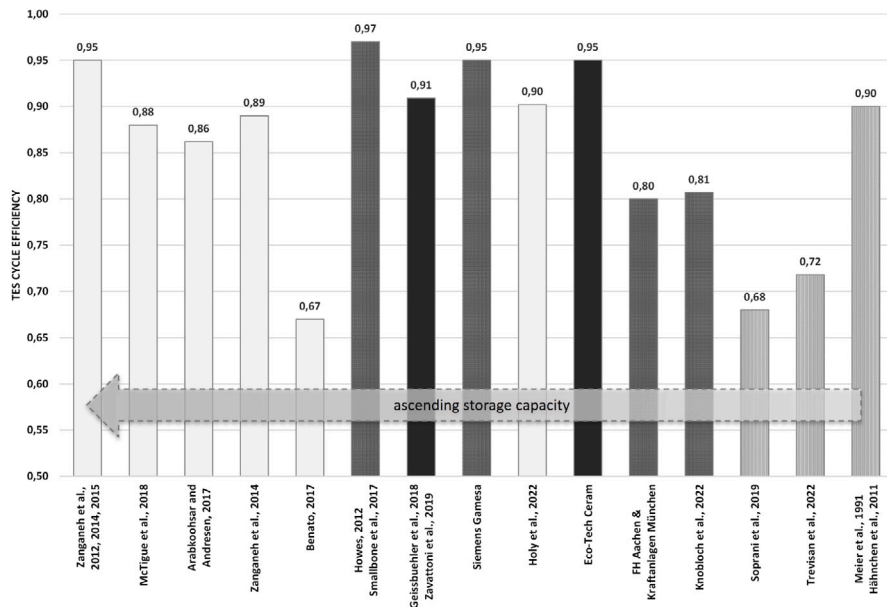


**Fig. 12.** Maximum TES cycle efficiencies from reported HTS-TES units. Arranged from right to left, according to ascending nominal storage capacity for theoretical concepts (unfilled) [35,39,89,102–104], lab-scale set ups (black-dotted) [86,98,99], demonstrators (white-dotted) [31,80,111–113] and pilot plants (filled) [93,101,109].

Trevisan [86] has investigated a storage with alumina as bulk storage material, which theoretically can be heated up to 1000 °C and has a volumetric heat capacity of about 480 Wh/(m³ K). The demonstrator presented by Lechner et al. [37] shows slightly higher values at about 530 Wh/(m³ K), this is due to the ceramic storage material consisting of a firebrick masonry stack. Its maximum temperature was specified as 1100 °C. Currently, a demonstrator with ceramic cast molded bricks is under construction in the research project FlexQuartier Gießen [39] of the University of Applied Sciences TH Mittelhessen. On the basis of the previous project, some characteristics like the geometry and the storage material were optimized. The volumetric capacity of the storage material will be about 550 Wh/(m³ K) and is supposed to be able to reach up to 1200 °C. It should be mentioned that these are direct electrically (internally) charged concepts. Thus, in contrast to PB storages, the non-usable capacity during charging is already considered in the specification of $c_{TES,vol}$ (see Section 3.2). Only the theoretical concept of Stack et al. [7] reaches higher temperatures of up to 1600 °C. It is the only

concept that is already in the ultra high temperature range. As in the case of Lechner et al. the storage material consists of fireclay bricks in a masonry bond and the volumetric capacity is approx. 700 Wh/(m³ K).

The reported thermal cycle efficiencies (TES cycle efficiencies) for S-TES are shown in Fig. 12. Most of the storage units show efficiencies above 80 percent, while those with efficiencies ≥ 95% are particularly noticeable. Among them is the concept of a truncated cone-shaped PB storage unit with 95% efficiency published by Zanganeh et al. [102]. Siemens Gamesa also reported an efficiency of 95% for their first demonstrator at the University of Hamburg-Harburg [111]. The construction system developed commercially by Isentropic ltd. [112] even reaches 97%. The resulting demonstrator was completed at Newcastle University and investigated by Smallbone et al. [113]. Eco-Tech Ceram has built a commercial pilot plant which they claim uses recycled bulk ceramic material and has an efficiency of 95% as well [109].

Three PB storage units, which are around 70% TES cycle efficiency also stand out. The first of them is the theoretical PTES-CB published

by Benato [35]. For these, a cycle efficiency of 67% was reported for the hot reservoir (HTS-TES), with an alpha alumina sphere filling. High losses at the heat exchanger during charging and low maximum temperatures during thermal cycling were specified as reasons for the low efficiency. The second storage is a demonstrator with volcanic rock bed from the Technical University of Denmark [79]. In this case, stratification problems (see Section 3.2) during charging and discharging were the cause. These were resolved in the next demonstrator by changing the design to a hemisphere, which increased the efficiency to up to 81% [80]. Trevisan et al. reported an efficiency of 72% due to thermocline spreading [86].

In summary, according to the state of the art, HTS-TES cycle efficiencies >80% can be achieved even for capacities in the MWh range, and with scaling effects efficiencies around 95% and more are possible.

## 5. Conclusions

This work classifies Carnot Batteries according to a new approach and positions the TES within them. A classification over the whole temperature range from below 0 °C up to over 1500 °C is presented, which allows to distinguish the high number of storage units in the high temperature range in particular. It gives an overview of solid and sensible high temperature energy storage units from literature and industry with a focus on solid storage materials, distinguishes by design and compares them based on key figures. The following conclusions can be drawn:

- Carnot Batteries can be grouped into Compressed Air Energy Storage Carnot Batteries (CAES CB), Liquid Air Energy Storage Carnot Batteries (LAES CB) and Thermal Energy Storage Carnot Batteries (TES CB). In terms of their charging method, they can be distinguished by the location of the energy conversion and the mechanism. In terms of their discharging method, the power conversion process is crucial.
- In terms of design type, sensible thermal energy storage with solid storage material can be divided into packed bed and fixed structure (for non-packed bed) and distinguished on the basis of the storage material used.
- The storage technology of high temperature sensible TES becomes more efficient with increasing storage size and cycle efficiencies from 80% to over 95% can be achieved.
- In addition to the material density, the classification of the operating temperature represents an important indication of the energetically and exergetically usable potential of a sensible TES. Most of the systems investigated so far are located in the lower third of the high-temperature range (600–900 °C) and are designed as externally charged packed bed storage systems. As a result, there is great need for research in the area of fixed structure TES with sensible storage material as part of a Carnot Battery, in particular for internally charged storage units in the upper high temperature range (>1000 °C). Until now, very few demonstrators have been built and few articles have been published in this research area, despite the great technological potential.
- The number of commercially developed systems is still small, but because of the high potential, research groups and companies around the world have started to embrace this technology in recent years and are pushing ahead with its development.

## Declaration of competing interest

The authors declare that they have no known competing financial interests or personal relationships that could have appeared to influence the work reported in this paper.

## Data availability

Data will be made available on request.

| Nomenclature | | |
|---|---|---|
| **Abbreviations** | | |
| CB | Carnot Battery | |
| CEAS | compressed air energy storage | |
| FS | fixed structure | |
| HE | heat engine | |
| HTS-TES | high temperature sensible energy storage | |
| HT-TES | high temperature thermal energy storage | |
| HTF | heat transfer fluid | |
| LAES | liquid air energy storage | |
| L-TES | latent thermal energy storage | |
| LT-TES | low temperature thermal energy storage | |
| MT-TES | medium temperature thermal energy storage | |
| PB | packed bed | |
| PTES | pumped thermal energy storage | |
| SoC | state of charge | |
| S-TES | sensible thermal energy storage | |
| TC-TES | thermo-chemical energy storage | |
| TES | thermal energy storage | |
| TPV | thermal photovoltaic | |
| UHT-TES | ultra-high temperature thermal energy storage | |
| **Thermodynamic properties** | | |
| $A$ | Area | [m$^2$] |
| $C_{ch,\ loss}$ | capacity of charging losses | [Wh] |
| $C_{dis,\ loss}$ | capacity of discharging losses | [Wh] |
| $c_{mat}$ | heat capacity of storage material | [J/(kg K)] |
| $\bar{c}_{mat}$ | average heat capacity storage material | [J/(kg K)] |
| $C_{nom}$ | nominal capacity | [MWh] |
| $c_{nom,vol}$ | nominal volumetric heat capacity of TES | [Wh/m$^3$] |
| $\bar{c}_{TES,vol}$ | volumetric heat capacity of TES | [Wh/(m$^3$ K)] |
| $C_{usable}$ | usable capacity | [Wh] |
| $D_h$ | hydraulic diameter | [m] |
| $E_{th}$ | thermal energy | [Wh] |
| $E_{th,c}$ | thermal energy of charging | [Wh] |
| $E_{th,d}$ | thermal energy of discharging | [Wh] |
| $m_{TES}$ | mass of TES | [t] |
| $P$ | Perimeter | [m] |
| $SoC_{TES}$ | state of charge | [–] |
| $T_{max}$ | maximal temperature | [° C] |
| $T_{max,\ ch,\ out}$ | maximal outlet temperature limit | [° C] |
| $T_{min}$ | minimal temperature | [° C] |
| $T_{min,\ dis,\ out}$ | minimal outlet temperature limit | [° C] |
| $T_{ref}$ | reference temperature | [° C] |
| $T_{TES}$ | temperature of TES | [° C] |
| $V_{void}$ | volume of void | [m$^3$] |
| $V_{mat}$ | volume of material | [m$^3$] |
| $V_{TES}$ | volume of TES | [m$^3$] |
| $\Delta T_{nom}$ | nominal temperature difference | [K] |
| $\Delta T_{TES}$ | temperature difference of TES | [K] |
| $\Delta U_{TES}$ | difference in inner energy of TES | [J] |
| $\Delta U_{TES,c}$ | difference in inner energy of TES during charging | [J] |
| $\Delta U_{TES,d}$ | difference in inner energy of TES during discharging | [J] |
| $\epsilon$ | void fraction | [–] |
| $\eta$ | thermal cycle efficiency | [–] |
| $\rho_{mat}$ | density of storage material | [kg/m$^3$] |
| $\Phi$ | usable capacity ratio | [–] |

**Table A.4**
Overview of solid HTS-TES from the literature sorted by ascending capacity.

| Source | Scale | $T_{max}$ | $\Delta T_{op}$ | Energy conversion | Shape | Main flow direction | Storage inventory | Volume | Material mass | $\bar{c}_{mat}$ | $\bar{c}_{TES,vol}$ | $C_{nom}$ | $\epsilon$ | $\eta_{TES}$ | Storage design |
|---|---|---|---|---|---|---|---|---|---|---|---|---|---|---|---|
| [-] | [-] | [° C] | [° C] | [-] | [-] | [-] | [-] | [m³] | [t] | [J/kg/K] | [Wh/(m³K)] | [MWh] | [-] | [%] | [-] |
| [61,97] | 1 | 700 | 20–120 | externally | cylinder | vertical | alpha alumina | 7.9E−04[a] | 2.0E−03[a] | 995[a] | 685[a] | 5.4E−05[a] | 0.38[a] | n.a. | PB |
| [98,99] | 1 | 700 | 20–550 | externally | cylinder | vertical | crushed steatite | 2.1E−02[a] | 3.3E−02[a] | 1068 | 477[a] | 9.8E−04[a] | 0.40 | 0.90 | PB |
| [94] | 1 | 680 | 58–500 | externally | cuboid | vertical | ceramic honeycomb bricks | 1.2E−01[a] | 1.5E−01[a] | 1000 | 341[a] | 1.8E−02[a] | 0.34 | n.a. | FS |
| [74] | 1 | 530 | 20–530 | externally | cuboid | vertical | ceramic plateswith cutouts | 1.1E−01[a] | 2.8E−01[a] | 800 | 569[a] | 1.9E−02[a] | 0.20 | n.a. | FS |
| [68] | 1 | 900 | 25–900 | externally | cylinder | vertical | Denstone ceramicpebbles | 7.8E−02[a] | 1.0E−01[a] | 1135[a] | 423[a] | 2.9E−02[a] | 0.39 | n.a. | PB |
| [86] | 1 | 1000 | 25–700 | externally | cylinder | radial | alpha alumina | 2.2E−01 | 3.0E−01 | 820 | 484[a] | 5.0E−02 | 0.39 | 0.72 | PB |
| [94] | 1 | 680 | 15–400 | externally | cuboid | vertical | ceramic honeycomb bricks | 1.04[a] | 0.77[a] | 869[a] | 179[a] | 7.1E−02[a] | 0.42 | n.a. | FS |
| [109] | 1 | 900 | ≤900 | externally | cylinder | horizontal | waste refractoryceramics | n.a. | n.a. | n.a. | n.a. | 8.0E−02 | n.a. | n.a. | n.a. |
| [100] | 1 | 530 | 20–530 | externally | cuboid | vertical | rocks (dolerite) | 1.50[a] | 3.00 | 815 | 453[a] | 4.0E−01 | 0.40 | n.a. | PB |
| [79] | 1 | 600 | 20–500 | externally | cuboid | horizontal | rocks | 1.50 | 2.48[a] | 960 | 441[a] | 4.5E−01 | 0.45 | 0.68 | PB |
| [80] | 2 | 600 | 20–500 | externally | hemisphere | vertical | crushed rocks | 3.20 | 5.39 | 1120 | 411[a] | 1.00 | 0.56[a] | 0.81 | PB |
| [108] | 1 | 1000 | ≤1000 | externally | cylinder | vertical | ceramic pbmaterial | n.a. | n.a. | n.a. | n.a. | 1.00 | n.a. | n.a. | PB |
| [60] | 2 | 900 | 20–700 | externally | cylinder | vertical | EAF steelslag pebbles | 3.00 | 6.48[a] | 877 | 526[a] | 1.05 | 0.37 | n.a. | PB |
| [95] | 3 | 800 | 80–800 | externally | cuboid | vertical | ceramic plates | 3.20 | 4.80[a] | 1001[a] | 417[a] | 1.11 | 0.40 | n.a. | FS |
| [31] | 2 | 1000 | ≤1000 | externally | cuboid | vertical | ceramic honeycombs | n.a. | n.a. | n.a. | n.a. | 1.40 | n.a. | 0.80 | FS |
| [95] | 3 | 800 | 80–800 | externally | cuboid | vertical | basalt pebbles | 3.56 | 6.62[a] | 973[a] | 502[a] | 1.42 | 0.37 | n.a. | PB |
| [8,110] | 2 | 600 | ≤500 | externally | cuboid | radial | small grainedsilica sand | 6.68[a] | 10.56 | 1300 | 571[a] | 1.50 | 0.40 | n.a. | PB |
| [37] | 2 | 1100 | 800–1050 | internally | cuboid | vertical | massiveceramic bricks | 11.57[a] | 18.10 | 1200 | 521[a] | 1.51[a] | 0.31 | n.a. | FS |
| [109] | 3 | 1000 | ≤600 | externally | cuboid | horizontal | waste refractoryceramics | n.a. | n.a. | n.a. | n.a. | 2.00 | n.a. | 0.95 | n.a. |
| [76] | 3 | 650 | ≤450 | externally | cuboid | horizontal | steel rods | n.a. | n.a. | n.a. | n.a. | 2.40 | n.a. | n.a. | FS |
| [74] | 0 | 650 | 350–650 | externally | cuboid | vertical | ceramic plateswith cutouts | 23.44[a] | 60.00[a] | 800 | 569[a] | 4.00 | 0.20 | n.a. | FS |
| [81] | 3 | 1300 | ≤500 | externally | cuboid | vertical | high temperatureconcrete granulate | n.a. | n.a. | n.a. | n.a. | 4.20 | n.a. | n.a. | PB |
| [39] | 0 | 1200 | 600–1200 | internally | cuboid | horizontal | ceramic plateswith cutouts | 14.52 | 28.70 | 1000 | 549[a] | 4.78 | 0.25 | 0.90 | FS |
| [111] | 2 | 800 | ≤600 | externally | cuboid | horizontal | crushed rock | n.a. | 40.00 | n.a. | n.a. | 5.00 | n.a. | 0.95 | PB |
| [28] | 2 | 680 | 120–680 | externally | cuboid | vertical | alumina porcelain,honeycomb bricks | 294.0[a] | 246.1[a] | 880 | 205[a] | 8.60 | 0.69 | n.a. | FS |
| [93,101] | 3 | 550 | 15–550 | externally | modifiedhalf cylinder | vertical | crushed rock | 44.00 | 76.29[a] | 1055[a] | 508[a] | 12.00 | 0.34 | 0.91 | PB |
| [112,113] | 2 | 500 | ≤500 | externally | cylinder | vertical | crushed rock | n.a. | n.a. | n.a. | n.a. | 16.00 | n.a. | 0.97 | PB |
| [35] | 0 | 550 | ≤550 | externally | cylinder | vertical | alpha aluminaspheres | 150.0 | 359.1[a] | 1082[a] | 720[a] | 26.98[a] | 0.40 | 0.67 | PB |
| [102] | 0 | 550 | 250–550 | externally | modifiedturncated cone | vertical | rocks | 324.1[a] | 1371.4[a] | 875[a] | 434[a] | 100.0 | 0.35 | 0.89 | PB |
| [103] | 0 | 677 | 600–677 | internally | cylinder | vertical | rocks | 4000.0 | 7020.0[a] | 862 | 403[a] | 124.0[a] | 0.35 | 0.86 | PB |
| [29,115] | 2 | 800 | ≤750 | externally | cuboid | horizontal | crushedvolcanic rock | 207.8[a] | 1000.0 | 982[a] | 496[a] | 130.0 | 0.39 | n.a. | PB |
| [104] | 0 | 500 | 50–500 | externally | cylinder | vertical | magnetiteparticles | 465.5 | 1445.4[a] | 874 | 754[a] | 160.0 | 0.40 | 0.88 | PB |
| [114] | 3 | 750 | ≤750 | externally | cuboid | horizontal | crushed rocks | 2304.0[a] | n.a. | n.a. | n.a. | 200.0 | n.a. | n.a. | PB |
| [7] | 0 | 1600 | 500–1200 | internally | n.a. | vertical | massiveceramic bricks | 177.0 | 529.2[a] | 840 | 698[a] | 250.0 | 0.25 | n.a. | FS |
| [26] | 0 | 900 | 120–700 | externally | cylinder | vertical | EAF steelslag pebbles | 2571.8[a] | 14702.3[a] | 933 | 533[a] | 2210.0 | 0.40 | n.a. | PB |
| [89,102] [105] | 0 | 650 | 150–650 | externally | modifiedturncated cone | vertical | rocks | 14253.6[a] | 59245.7[a] | 875[a] | 437[a] | 7200.0 | 0.34 | 0.95 | PB |
| [116] | 3 | 1000 | ≤1000 | externally | cuboid | vertical | sands | n.a. | n.a. | n.a. | n.a. | n.a. | n.a. | n.a. | PB |
| [117] | 0 | 1200 | ≤1000 | externally | cylinder | vertical | silica sands | n.a. | n.a. | n.a. | n.a. | n.a. | n.a. | n.a. | PB |
| [118] | 3 | 600 | 75–600 | externally | cylinder | vertical | crushed rocks | n.a. | n.a. | n.a. | n.a. | n.a. | n.a. | n.a. | PB |
| [82] | 2 | 1000 | ≤1000 | externally | cuboid | horizontal | silica sand | n.a. | n.a. | n.a. | n.a. | n.a. | n.a. | n.a. | PB |
| [75] | 0 | 2000 | ≤1600 | internally | cylinder | vertical | ceramichoneycomb cowperstones | n.a. | n.a. | n.a. | n.a. | n.a. | n.a. | n.a. | FS |
| [119] | 0 | 1500 | ≤1500 | internally | cuboid | none | graphite blocks | n.a. | n.a. | n.a. | n.a. | n.a. | n.a. | n.a. | FS |
| [72] | 2 | 600 | ≤600 | externally | cuboid | horizontal | high temperatureconcrete with inner tubes | n.a. | n.a. | n.a. | n.a. | n.a. | n.a. | n.a. | FS |
| [106] | 1 | 1100 | ≤960 | externally | cylinder | vertical | zirconiumoxide pallets | 0.13[a] | 0.47[a] | n.a. | n.a. | n.a. | 0.32 | n.a. | PB |

## Appendix

See Table A.4.

## References

[1] BMUV, National climate policy of Germany, 2022, Federal Ministry for the Environment, Nature Conservation, Nuclear Safety and Consumer Protection - National Climate Policy. https://www.bmuv.de/en/topics/climate-adaptation/climate-protection/national-climate-policy.

[2] Sixth Assessement Report on Climate Change (IPCC), 2022, https://www.ipcc.ch/report/sixth-assessment-report-working-group-i/.

[3] IRENA, World Energy Transitions Outlook: 1.5°C Pathway, International Renewable Energy Agency (IRENA), Abu Dhabi, United Arab Emirates, 2022.

[4] Z. Topalović, R. Haas, A. Ajanović, A. Hiesl, Economics of electric energy storage. The case of Western Balkans, Energy 238 (2022) 121669, http://dx.doi.org/10.1016/j.energy.2021.121669.

[5] statista Handelsblatt, Kapazität von Großbatteriespeichern zur Netzstabilisierung in Deutschland in den Jahren von 2015 bis 2018, 2022, Statista. https://de.statista.com/statistik/daten/studie/872079/umfrage/kapazitaet-von-grossbatteriespeichern-zur-netzstabilisierung-in-deutschland/.

[6] A.V. Olympios, J.D. McTigue, P. Sapin, C.N. Markides, Pumped-Thermal Electricity Storage Based on Brayton Cycles, in: Reference Module in Earth Systems and Environmental Sciences, Elsevier, 2021, http://dx.doi.org/10.1016/B978-0-12-819723-3.00086-X, B978012819723300086X.

[7] D.C. Stack, D. Curtis, C. Forsberg, Performance of firebrick resistance-heated energy storage for industrial heat applications and round-trip electricity storage, Appl. Energy 242 (2019) 782–796, http://dx.doi.org/10.1016/j.apenergy.2019.03.100.

[8] G. Schneider, H. Maier, J. Häcker, S. Siegele, Electricity Storage With a Solid Bed High Temperature Thermal Energy Storage System (HTTES) - A Methodical Approach to Improve the Pumped Thermal Grid Storage Concept:, in: 14th International Renewable Energy Storage Conference 2020, IRES 2020, Bonn, Germany, 2021, http://dx.doi.org/10.2991/ahe.k.210202.005.

[9] IRENA, Innovation Outlook: Thermal Energy Storage, International Renewable Energy Agency (IRENA), Abu Dhabi, United Arab Emirates, 2020.

[10] A. Olabi, C. Onumaegbu, T. Wilberforce, M. Ramadan, M.A. Abdelkareem, A.H. Al - Alami, Critical review of energy storage systems, Energy 214 (2021) 118987, http://dx.doi.org/10.1016/j.energy.2020.118987.

[11] C.K. Das, O. Bass, G. Kothapalli, T.S. Mahmoud, D. Habibi, Overview of energy storage systems in distribution networks: Placement, sizing, operation, and power quality, Renew. Sustain. Energy Rev. 91 (2018) 1205–1230, http://dx.doi.org/10.1016/j.rser.2018.03.068.

[12] O. Dumont, G.F. Frate, A. Pillai, S. Lecompte, M. De paepe, V. Lemort, Carnot battery technology: A state-of-the-art review, J. Energy Storage 32 (2020) 101756, http://dx.doi.org/10.1016/j.est.2020.101756.

[13] V. Novotny, V. Basta, P. Smola, J. Spale, Review of Carnot Battery Technology Commercial Development, Energies 15 (2) (2022) 647, http://dx.doi.org/10.3390/en15020647.

[14] T. Esence, A. Bruch, S. Molina, B. Stutz, J.-F. Fourmigué, A review on experience feedback and numerical modeling of packed-bed thermal energy storage systems, Sol. Energy 153 (2017) 628–654, http://dx.doi.org/10.1016/j.solener.2017.03.032.

[15] J. Gasia, L. Miró, L.F. Cabeza, Review on system and materials requirements for high temperature thermal energy storage. Part 1: General requirements, Renew. Sustain. Energy Rev. 75 (2017) 1320–1338, http://dx.doi.org/10.1016/j.rser.2016.11.119.

[16] A. Gil, M. Medrano, I. Martorell, A. Lázaro, P. Dolado, B. Zalba, L.F. Cabeza, State of the art on high temperature thermal energy storage for power generation. Part 1—Concepts, materials and modellization, Renew. Sustain. Energy Rev. 14 (1) (2010) 31–55, http://dx.doi.org/10.1016/j.rser.2009.07.035.

[17] M. Medrano, A. Gil, I. Martorell, X. Potau, L.F. Cabeza, State of the art on high-temperature thermal energy storage for power generation. Part 2—Case studies, Renew. Sustain. Energy Rev. 14 (1) (2010) 56–72, http://dx.doi.org/10.1016/j.rser.2009.07.036.

[18] T. Liang, A. Vecchi, K. Knobloch, A. Sciacovelli, K. Engelbrecht, Y. Li, Y. Ding, Key components for Carnot Battery: Technology review, technical barriers and selection criteria, Renew. Sustain. Energy Rev. 163 (2022) 112478, http://dx.doi.org/10.1016/j.rser.2022.112478.

[19] I.T.C. Programme, G.A. Center, IEA Energy Storage TASK 36 - Carnot Batteries, 2022, https://www.eces-a36.org/.

[20] W.-D. Steinmann, Thermo-mechanical concepts for bulk energy storage, Renew. Sustain. Energy Rev. 75 (2017) 205–219, http://dx.doi.org/10.1016/j.rser.2016.10.065.

[21] J. Lizana, R. Chacartegui, A. Barrios-Padura, J.M. Valverde, C. Ortiz, Identification of best available thermal energy storage compounds for low-to-moderate temperature storage applications in buildings, Mater. Constr. 68 (331) (2018) 160, http://dx.doi.org/10.3989/mc.2018.10517.

[22] T. Bauer, W.-D. Steinmann, D. Laing, R. Tamme, Thermal energy storage materials and systems, Ann. Rev. Heat Transfer 15 (15) (2012) 131–177, http://dx.doi.org/10.1615/AnnualRevHeatTransfer.2012004651.

[23] P. Tatsidjodoung, N. Le Pierrès, L. Luo, A review of potential materials for thermal energy storage in building applications, Renew. Sustain. Energy Rev. 18 (2013) 327–349, http://dx.doi.org/10.1016/j.rser.2012.10.025.

[24] L. Miró, J. Gasia, L.F. Cabeza, Thermal energy storage (TES) for industrial waste heat (IWH) recovery: A review, Appl. Energy 179 (2016) 284–301, http://dx.doi.org/10.1016/j.apenergy.2016.06.147.

[25] S. Puschnigg, J. Lindorfer, S. Moser, T. Kienberger, Techno-economic aspects of increasing primary energy efficiency in industrial branches using thermal energy storage, J. Energy Storage 36 (2021) 102344, http://dx.doi.org/10.1016/j.est.2021.102344.

[26] M. Krüger, S. Muslubas, T. Loeper, F. Klasing, P. Knödler, C. Mielke, Potentials of Thermal Energy Storage Integrated into Steam Power Plants, Energies 13 (9) (2020) 2226, http://dx.doi.org/10.3390/en13092226.

[27] D. Laing, D. Lehmann, M. Fiß, C. Bahl, Test Results of Concrete Thermal Energy Storage for Parabolic Trough Power Plants, J. Solar Energy Eng. 131 (4) (2009) 041007, http://dx.doi.org/10.1115/1.3197844.

[28] S. Zunft, M. Hänel, M. Krüger, V. Dreißigacker, F. Göhring, E. Wahl, Jülich Solar Power Tower—Experimental Evaluation of the Storage Subsystem and Performance Calculation, J. Solar Energy Eng. 133 (3) (2011) 031019, http://dx.doi.org/10.1115/1.4004358.

[29] M. von der Heyde, G. Schmitz, Electric Thermal Energy Storage Based on Packed Bed, in: Encyclopedia of Energy Storage, 2022, pp. 108–121, http://dx.doi.org/10.1016/B978-0-12-819723-3.00053-6.

[30] E.S. TCP, IEA Technology Collaboration Programme Newsletter, 2022, IEA. https://mailchi.mp/3fdf3c968490/iea-es-tcp-newsletter-september-2021?e=4b98bf90a8.

[31] S. Jülich, multiTESS – Store Energy Congress, 2022, Kraftanlagen Energies & Services GmbH. https://www.storenergy.de/sites/storenergy.de/files/media_document/2021-10/rabea_dluhosch_abstract_2021.pdf.

[32] A. Robinson, Ultra-high temperature thermal energy storage. Part 1: Concepts, J. Energy Storage 13 (2017) 277–286, http://dx.doi.org/10.1016/j.est.2017.07.020.

[33] A. Robinson, Ultra-high temperature thermal energy storage. Part 2: Engineering and operation, J. Energy Storage 18 (2018) 333–339, http://dx.doi.org/10.1016/j.est.2018.03.013.

[34] L. Sanz Garcia, E. Jacquemoud, P. Jenny, Thermo-economic heat exchanger optimization for Electro-Thermal Energy Storage based on transcritical CO2 cycles, in: Conference Proceedings of the European SCO2 Conference3rd European Conference on Supercritical CO2 (SCO2) Power Systems 2019: 19th-20th September 2019, DuEPublico: Duisburg-Essen Publications online, University of Duisburg-Essen, Germany, 2019, p. 353, http://dx.doi.org/10.17185/DUEPUBLICO/48917.

[35] A. Benato, Performance and cost evaluation of an innovative Pumped Thermal Electricity Storage power system, Energy 138 (2017) 419–436, http://dx.doi.org/10.1016/j.energy.2017.07.066.

[36] P. Peng, L. Yang, A. Menon, N. Weger, R. Prasher, H. Breunig, S. Lubner, Techno-Economic Analysis of High-Temperature Thermal Energy Storage for On-Demand Heat and Power, 2022, p. 18, http://dx.doi.org/10.26434/chemrxiv-2022-3l03r-v2.

[37] S. Lechner, K. Behler, F. Holy, D. Thölken, T. Ascher, F. von der Grün, M. Richter, Sektorenübergreifender Hochtemperaturspeicher zum Ausgleich volatiler erneuerbarer Stromerzeugung, 2020, http://dx.doi.org/10.2314/KXP:1745063919.

[38] F. Holy, M. Textor, S. Lechner, Gas turbine cogeneration concepts for the pressureless discharge of high temperature thermal energy storage units, J. Energy Storage (2021) 11, http://dx.doi.org/10.1016/j.est.2021.103283.

[39] F. Holy, A. Paul, M. Textor, S. Lechner, N. Metka, F. Klaus, Sensibler Hochtemperaturspeicher bis 1200°C mit extern beheiztem Gasturbinenprozess - Entwicklung und Simulation einer neuartigen Carnot-Batterie zur dezentralen Sektorenkopplung, in: Kraftwerkstechnik, Vol. 54, Saxonia, Dresden, Germany.

[40] M. Gong, F. Ottermo, High-temperature thermal storage in combined heat and power plants, Energy 252 (2022) 124057, http://dx.doi.org/10.1016/j.energy.2022.124057.

[41] S. Jülich, Energy Storage Projects; TESS 2.0, 2021, https://www.fh-aachen.de/en/research/solar-institute-juelich/focus-areas/projects-energy-storage/.

[42] S. Trevisan, R. Guédez, B. Laumert, Thermo-economic optimization of an air driven supercritical CO2 Brayton power cycle for concentrating solar power plant with packed bed thermal energy storage, Sol. Energy 211 (2020) 1373–1391, http://dx.doi.org/10.1016/j.solener.2020.10.069.

[43] J. Yang, Z. Yang, Y. Duan, Off-design performance of a supercritical CO2 Brayton cycle integrated with a solar power tower system, Energy 201 (2020) 117676, http://dx.doi.org/10.1016/j.energy.2020.117676.

[44] A. Benato, A. Stoppato, Heat transfer fluid and material selection for an innovative Pumped Thermal Electricity Storage system, Energy 147 (2018) 155–168, http://dx.doi.org/10.1016/j.energy.2018.01.045.

[45] S. Houssainy, M. Janbozorgi, P. Kavehpour, Thermodynamic performance and cost optimization of a novel hybrid thermal-compressed air energy storage system design, J. Energy Storage 18 (2018) 206–217, http://dx.doi.org/10.1016/j.est.2018.05.004.

[46] M. Mahmood, A. Traverso, A.N. Traverso, A.F. Massardo, D. Marsano, C. Cravero, Thermal energy storage for CSP hybrid gas turbine systems: Dynamic modelling and experimental validation, Appl. Energy 212 (2018) 1240–1251, http://dx.doi.org/10.1016/j.apenergy.2017.12.130.

[47] D. Stevanovic, High Temperature Energy Storage (HiTES) with Pebble Heater Technology and Gas Turbine, in: X. Chen, W. Cao (Eds.), Advancements in Energy Storage Technologies, InTech, 2018, http://dx.doi.org/10.5772/intechopen.75093.

[48] M.H. Nabat, M. Zeynalian, A.R. Razmi, A. Arabkoohsar, M. Soltani, Energy, exergy, and economic analyses of an innovative energy storage system; liquid air energy storage (LAES) combined with high-temperature thermal energy storage (HTES), Energy Convers. Manage. 226 (2020) 113486, http://dx.doi.org/10.1016/j.enconman.2020.113486.

[49] C. Amy, H.R. Seyf, M.A. Steiner, D.J. Friedman, A. Henry, Thermal energy grid storage using multi-junction photovoltaics, Energy Environ. Sci. 12 (1) (2019) 334–343, http://dx.doi.org/10.1039/C8EE02341G.

[50] N. Pfleger, T. Bauer, C. Martin, M. Eck, A. Wörner, Thermal energy storage – overview and specific insight into nitrate salts for sensible and latent heat storage, Beilstein J. Nanotechnol. 6 (2015) 1487–1497, http://dx.doi.org/10.3762/bjnano.6.154.

[51] F. Scheffler, Thermische Energiespeicher – Trends, Entwicklungen und Herausforderungen, Chem. Ing. Tech. 91 (9) (2019) 1219–1228, http://dx.doi.org/10.1002/cite.201800156.

[52] J. Pereira da Cunha, P. Eames, Thermal energy storage for low and medium temperature applications using phase change materials – A review, Appl. Energy 177 (2016) 227–238, http://dx.doi.org/10.1016/j.apenergy.2016.05.097.

[53] A.K. Ray, D. Rakshit, K. Ravi Kumar, H. Gurgenci, A Comparative Study of High-Temperature Latent Heat Storage Systems, Energies 14 (21) (2021) 6886, http://dx.doi.org/10.3390/en14216886.

[54] D. Fernandes, F. Pitié, G. Cáceres, J. Baeyens, Thermal energy storage: "How previous findings determine current research priorities", Energy 39 (1) (2012) 246–257, http://dx.doi.org/10.1016/j.energy.2012.01.024.

[55] P. Rundel, B. Meyer, M. Meiller, I. Meyer, R. Daschner, M. Jakuttis, M. Franke, S. Binder, A. Hornung, Fraunhofer UMSICHT Studie, Speicher Für Die Energiewende, Fraunhofer Institute for Environmental, Safety, and Energy Technology UMSICHT, 2013, http://dx.doi.org/10.13140/RG.2.2.14493.67048.

[56] A. Kallert, E. Lamvers, Y. JaeYu, Dena-Studie, Thermische Energiespeicher für Quartiere, Überblick Zu Rahmenbedingungen, Marktsituation Und Technologieoptionen Für Planung, Beratung Und Politische Entscheidungen Im Gebäudesektor, Deutsche Energie-Agentur GmbH (dena), 2021.

[57] N. Yu, R. Wang, L. Wang, Sorption thermal storage for solar energy, Prog. Energy Combust. Sci. 39 (5) (2013) 489–514, http://dx.doi.org/10.1016/j.pecs.2013.05.004.

[58] A. Sharma, V. Tyagi, C. Chen, D. Buddhi, Review on thermal energy storage with phase change materials and applications, Renew. Sustain. Energy Rev. 13 (2) (2009) 318–345, http://dx.doi.org/10.1016/j.rser.2007.10.005.

[59] M. Alonso, J. Vera-Agullo, L. Guerreiro, V. Flor-Laguna, M. Sanchez, M. Collares-Pereira, Calcium aluminate based cement for concrete to be used as thermal energy storage in solar thermal electricity plants, Cem. Concr. Res. 82 (2016) 74–86, http://dx.doi.org/10.1016/j.cemconres.2015.12.013.

[60] I. Ortega-Fernández, J. Rodríguez-Aseguinolaza, Thermal energy storage for waste heat recovery in the steelworks: The case study of the REslag project, Appl. Energy 237 (2019) 708–719, http://dx.doi.org/10.1016/j.apenergy.2019.01.007.

[61] R. Anderson, S. Shiri, H. Bindra, J.F. Morris, Experimental results and modeling of energy storage and recovery in a packed bed of alumina particles, Appl. Energy 119 (2014) 521–529, http://dx.doi.org/10.1016/j.apenergy.2014.01.030.

[62] V.A. Salomoni, C.E. Majorana, G.M. Giannuzzi, A. Miliozzi, R. Di Maggio, F. Girardi, D. Mele, M. Lucentini, Thermal storage of sensible heat using concrete modules in solar power plants, Sol. Energy 103 (2014) 303–315, http://dx.doi.org/10.1016/j.solener.2014.02.022.

[63] C.R. Jegathese, K.K. Murugavel, Analysis of Cooling Applications for Solar ThermalEnergy-Storage System, Appl. Math. Inf. Sci. 13 (2) (2019) 265–270, http://dx.doi.org/10.18576/amis/130214.

[64] C. Odenthal, W.-D. Steinmann, S. Zunft, Analysis of a horizontal flow closed loop thermal energy storage system in pilot scale for high temperature applications – Part I: Experimental investigation of the plant, Appl. Energy 263 (2020) 114573, http://dx.doi.org/10.1016/j.apenergy.2020.114573.

[65] C. Odenthal, W.-D. Steinmann, S. Zunft, Analysis of a horizontal flow closed loop thermal energy storage system in pilot scale for high temperature applications – Part II: Numerical investigation, Appl. Energy 263 (2020) 114576, http://dx.doi.org/10.1016/j.apenergy.2020.114576.

[66] R. Roy, D. Das, P.K. Rout, A Review of Advanced Mullite Ceramics, Eng. Sci. 18 (2022) 11, http://dx.doi.org/10.30919/es8d582.

[67] E.C. Nsofor, Investigations on the Packed Bed for High-Temperature Thermal Energy Storage, Int. J. Green Energy 17, http://dx.doi.org/10.1080/01971520500287925.

[68] P. Klein, T. Roos, T. Sheer, Experimental Investigation into a Packed Bed Thermal Storage Solution for Solar Gas Turbine Systems, Energy Procedia 49 (2014) 840–849, http://dx.doi.org/10.1016/j.egypro.2014.03.091.

[69] D. Laing, W.-D. Steinmann, R. Tamme, C. Richter, Solid media thermal storage for parabolic trough power plants, Sol. Energy 80 (10) (2006) 1283–1289, http://dx.doi.org/10.1016/j.solener.2006.06.003.

[70] D. Laing, C. Bahl, T. Bauer, D. Lehmann, W.-D. Steinmann, Thermal energy storage for direct steam generation, Sol. Energy 85 (4) (2011) 627–633, http://dx.doi.org/10.1016/j.solener.2010.08.015.

[71] N. Hoivik, C. Greiner, J. Barragan, A.C. Iniesta, G. Skeie, P. Bergan, P. Blanco-Rodriguez, N. Calvet, Long-term performance results of concrete-based modular thermal energy storage system, J. Energy Storage 24 (2019) 100735, http://dx.doi.org/10.1016/j.est.2019.04.009.

[72] S. Power, BolderBloc - Concrete Thermal Energy Storage, 2022, Storworks Power. https://storworks.com/our-technology/.

[73] W.-D. Steinmann, Development of Innovative Components for the CellFlux Storage Concept, in: SolarPACES, Vol. 18, Marrakech, Morocco, 11, p. 10, http://dx.doi.org/10.1115/1.4024921.

[74] S. Kuravi, J. Trahan, Y. Goswami, C. Jotshi, E. Stefanakos, N. Goel, Investigation of a High-Temperature Packed-Bed Sensible Heat Thermal Energy Storage System With Large-Sized Elements, J. Solar Energy Eng. 135 (4) (2013) 041008, http://dx.doi.org/10.1115/1.4023969.

[75] E.T.S. Inc., Decarbonizing Industry with renewable Heat, in: Electrified Thermal Solutions, 2022, https://www.electrifiedthermal.com/.

[76] L. GmbH, High-temperature steel storage - Menion, 2022, Lumenion. https://lumenion.com/?lang=en.

[77] H. Fricker, Regenerative thermal storage in atmospheric air system solar power plants, Energy 29 (5–6) (2004) 871–881, http://dx.doi.org/10.1016/S0360-5442(03)00192-0.

[78] K. Knobloch, T. Ulrich, C. Bahl, K. Engelbrecht, Degradation of a rock bed thermal energy storage system, Appl. Therm. Eng. 214 (2022) 118823, http://dx.doi.org/10.1016/j.applthermaleng.2022.118823.

[79] S. Soprani, F. Marongiu, L. Christensen, O. Alm, K.D. Petersen, T. Ulrich, K. Engelbrecht, Design and testing of a horizontal rock bed for high temperature thermal energy storage, Appl. Energy 251 (2019) 113345, http://dx.doi.org/10.1016/j.apenergy.2019.113345.

[80] K. Knobloch, Y. Muhammad, M.S. Costa, F.M. Moscoso, C. Bahl, O. Alm, K. Engelbrecht, A partially underground rock bed thermal energy storage with a novel air flow configuration, Appl. Energy 315 (2022) 118931, http://dx.doi.org/10.1016/j.apenergy.2022.118931.

[81] K. GmbH, Kraftblock Storage System, 2022, Kraftblock GmbH. https://kraftblock.com/en/applications/industrial-heat.html.

[82] M.G.E. SRL, Magaldi Green Thermal Energy Storage (MGTES), in: Magaldi Green Energy, 2022, https://www.magaldigreenenergy.com/en/mgtes-magaldi-green-thermal-energy-storage.

[83] M. Cascetta, F. Serra, G. Cau, P. Puddu, Comparison between experimental and numerical results of a packed-bed thermal energy storage system in continuous operation, Energy Procedia 148 (2018) 234–241, http://dx.doi.org/10.1016/j.egypro.2018.08.073.

[84] C. Odenthal, Analyse Und Demonstration Des CellFlux-Speichersystems, Universität Stuttgart, Stuttgart, 2015.

[85] M. Krüger, J. Haunstetter, J. Hahn, P. Knödler, S. Zunft, Development of Steelmaking Slag Based Solid Media Heat Storage for Solar Power Tower Using Air as Heat Transfer Fluid: The Results of the Project REslag, Energies 13 (22) (2020) 6092, http://dx.doi.org/10.3390/en13226092.

[86] S. Trevisan, W. Wang, R. Guedez, B. Laumert, Experimental evaluation of an innovative radial-flow high-temperature packed bed thermal energy storage, Appl. Energy 311 (2022) 118672, http://dx.doi.org/10.1016/j.apenergy.2022.118672.

[87] A. Bruch, S. Molina, T. Esence, J. Fourmigué, R. Couturier, Experimental investigation of cycling behaviour of pilot-scale thermal oil packed-bed thermal storage system, Renew. Energy 103 (2017) 277–285, http://dx.doi.org/10.1016/j.renene.2016.11.029.

[88] G. Zanganeh, High-Temperature Thermal Energy Storage for Concentrated Solar Power with Air as Heat Transfer Fluid, 2014, http://dx.doi.org/10.3929/ETHZ-A-010280563.

[89] G. Zanganeh, A. Pedretti, S. Zavattoni, M. Barbato, A. Steinfeld, Packed-bed thermal storage for concentrated solar power – Pilot-scale demonstration and industrial-scale design, Sol. Energy 86 (10) (2012) 3084–3098, http://dx.doi.org/10.1016/j.solener.2012.07.019.

[90] T.R. Davenne, S.D. Garvey, B. Cardenas, J.P. Rouse, Stability of packed bed thermoclines, J. Energy Storage 19 (2018) 192–200, http://dx.doi.org/10.1016/j.est.2018.07.015.

[91] V. Kronhardt, S. Alexopoulos, M. Reißel, J. Sattler, B. Hoffschmidt, M. Hänel, T. Doerbeck, High-temperature Thermal Storage System for Solar Tower Power Plants with Open-volumetric Air Receiver Simulation and Energy Balancing of a Discretized Model, Energy Procedia 49 (2014) 870–877, http://dx.doi.org/10.1016/j.egypro.2014.03.094.

[92] S. Trevisan, High-Temperature Thermal Energy Storage: A Comprehensive Study from Material Investigation to System Analysis Via Innovative Component Design, KTH, Stockholm, 2022.

[93] L. Geissbühler, V. Becattini, G. Zanganeh, S. Zavattoni, M. Barbato, A. Haselbacher, A. Steinfeld, Pilot-scale demonstration of advanced adiabatic compressed air energy storage, Part 1: Plant description and tests with sensible thermal-energy storage, J. Energy Storage 17 (2018) 129–139, http://dx.doi.org/10.1016/j.est.2018.02.004.

[94] Q. Li, F. Bai, B. Yang, Y. Wang, L. Xu, Z. Chang, Z. Wang, B. El Hefni, Z. Yang, S. Kubo, H. Kiriki, M. Han, Dynamic simulations of a honeycomb ceramic thermal energy storage in a solar thermal power plant using air as the heat transfer fluid, Appl. Therm. Eng. 129 (2018) 636–645, http://dx.doi.org/10.1016/j.applthermaleng.2017.10.063.

[95] T. Esence, T. Desrues, J.-F. Fourmigué, G. Cwicklinski, A. Bruch, B. Stutz, Experimental study and numerical modelling of high temperature gas/solid packed-bed heat storage systems, Energy 180 (2019) 61–78, http://dx.doi.org/10.1016/j.energy.2019.05.012.

[96] E. Comission, 2017_report_horizon 2020_working Programme.Pdf.

[97] R. Anderson, L. Bates, E. Johnson, J.F. Morris, Packed bed thermal energy storage: A simplified experimentally validated model, J. Energy Storage 4 (2015) 14–23, http://dx.doi.org/10.1016/j.est.2015.08.007.

[98] A. Meier, C. Winkler, D. Wuillemin, Experiment for modeling high temperature rock bed storage, Solar Energy Mater. 24 (1) (1991) 56–72, http://dx.doi.org/10.1016/0165-1633(91)90066-T.

[99] M. Hänchen, S. Brückner, A. Steinfeld, High-temperature thermal storage using a packed bed of rocks – Heat transfer analysis and experimental validation, Appl. Therm. Eng. 31 (10) (2011) 1798–1806, http://dx.doi.org/10.1016/j.applthermaleng.2010.10.034.

[100] K. Allen, T. von Backström, D. Kröger, Rock bed pressure drop and heat transfer: Simple design correlations, Sol. Energy 115 (2015) 525–536, http://dx.doi.org/10.1016/j.solener.2015.02.029.

[101] S.A. Zavattoni, L. Geissbühler, G. Zanganeh, A. Haselbacher, A. Steinfeld, M.C. Barbato, CFD modeling and experimental validation of the TES unit integrated into the world's first underground AA-CAES pilot plant, in: SOLARPACES 2018: International Conference on Concentrating Solar Power and Chemical Energy Systems, Casablanca, Morocco, 2019, http://dx.doi.org/10.1063/1.5117748, 200033.

[102] G. Zanganeh, G. Ambrosetti, A. Pedretti, S. Zavattoni, M. Barbato, P. Good, A. Haselbacher, A. Steinfeld, A 3 MWth parabolic trough CSP plant operating with air at up to 650°C, in: 2014 International Renewable and Sustainable Energy Conference (IRSEC), IEEE, Ouarzazate, Morocco, 2014, pp. 108–113, http://dx.doi.org/10.1109/IRSEC.2014.7059884.

[103] A. Arabkoohsar, G. Andresen, Dynamic energy, exergy and market modeling of a High Temperature Heat and Power Storage System, Energy 126 (2017) 430–443, http://dx.doi.org/10.1016/j.energy.2017.03.065.

[104] J.D. McTigue, C.N. Markides, A.J. White, Performance response of packed-bed thermal storage to cycle duration perturbations, J. Energy Storage 19 (2018) 379–392, http://dx.doi.org/10.1016/j.est.2018.08.016.

[105] G. Zanganeh, A. Pedretti, A. Haselbacher, A. Steinfeld, Design of packed bed thermal energy storage systems for high-temperature industrial process heat, Appl. Energy 137 (2015) 812–822, http://dx.doi.org/10.1016/j.apenergy.2014.07.110.

[106] A.A. Jalalzadeh-Azar, W.G. Steele, G.A. Adebiyi, Heat Transfer in a High-Temperature Packed Bed Thermal Energy Storage System—Roles of Radiation and Intraparticle Conduction, J. Energy Resour. Technol. 118 (1) (1996) 50–57, http://dx.doi.org/10.1115/1.2792693.

[107] A. Arabkoohsar, G. Andresen, Design and analysis of the novel concept of high temperature heat and power storage, Energy 126 (2017) 21–33, http://dx.doi.org/10.1016/j.energy.2017.03.001.

[108] C.C.T. GmbH, T. GmbH, Safr Project - Carbon Clean Carnot Battery, 2022, CarbonClean Technologies GmbH. http://www.safr-project.org/.

[109] E.T. Ceram, Energy Storage, 2022, ETC Eco-Tech Ceram. https://ecotechceram.com/en/the-company/.

[110] D. Schlipf, E. Faust, G. Schneider, H. Maier, First operational results of a high temperature energy storage with packed bed and integration potential in CSP plants, in: SOLARPACES 2016: International Conference on Concentrating Solar Power and Chemical Energy Systems, Abu Dhabi, United Arab Emirates, 2017, http://dx.doi.org/10.1063/1.4984445, 080024.

[111] S. Gamesa, Vortrag Windernergietage 2017 - ETES Siemens Gamesa, 2022, https://windenergietage.de/wp-content/uploads/sites/2/2017/11/26WT0811_F11_1120_Dr_Barmeier.pdf.

[112] J. Howes, Concept and Development of a Pumped Heat Electricity Storage Device, Proc. IEEE 100 (2) (2012) 493–503, http://dx.doi.org/10.1109/JPROC.2011.2174529.

[113] A. Smallbone, V. Jülch, R. Wardle, A.P. Roskilly, Levelised Cost of Storage for Pumped Heat Energy Storage in comparison with other energy storage technologies, Energy Convers. Manage. 152 (2017) 221–228, http://dx.doi.org/10.1016/j.enconman.2017.09.047.

[114] B. Energy, bGen - Carbon-Free Thermal Energy Storage, 2022, Brenmiller Energy. https://bren-energy.com/utility-tes/.

[115] M. von der Heyde, Electric Thermal Energy Storage Based on Packed Beds for Renewable Energy Integration (Ph.D. thesis), TUHH Universitätsbibliothek, 2022, http://dx.doi.org/10.15480/882.4165.

[116] B.N. Anderson, Modular Solar Systems for 24/7 Scalable, Flexible, Affordable Electricity, in: ASME Power Conference, American Society of Mechanical Engineers, Charlotte, North Carolina, USA, 2017, http://dx.doi.org/10.1115/POWER-ICOPE2017-3155, V002T09A002.

[117] J. Gifford, Z. Ma, P. Davenport, Thermal Analysis of Insulation Design for a Thermal Energy Storage Silo Containment for Long-Duration Electricity Storage, Front. Energy Res. 8 (2020) 99, http://dx.doi.org/10.3389/fenrg.2020.00099.

[118] S. A/S, GridScale Energy Storage System, 2022, Stiesdal. https://www.stiesdal.com/wp-content/uploads/2021/11/30883-Stiesdal-Storage-Technologies-brochure.pdf.

[119] A. Energy, Solid State Thermal Battery with High Energy Density, Long Duration, and Low Maintenance. Antora Energy. https://reimaginingenergy.afwerx.com/exhibitor/antora-energy-11612/.

[120] BMWI, Newsletter BMWI - Siemens Gamesa ETES, 2022, Newsletter BMWI - Vulkangestein Speichert Windstrom. https://www.bmwi-energiewende.de/EWD/Redaktion/Newsletter/2019/07/Meldung/News1.html.